Theoretical and numerical analysis of different modes in a system of a "kicked" magnetic pendulum

Krystian Polczyński, Adam Wijata, Jan Awrejcewicz

Abstract: A non-linear magnetic pendulum system has been studied theoretically and numerically. The main component of the system is a pendulum equipped with a neodymium magnet, which is "kicked" by an alternating magnetic field form an electrical coil underneath. The current signal which flows through the coil is repeatedly switched on and off with a given frequency and a duty cycle. Switched on magnetic field introduces a two-well potential instead of a single-well gravitational one, what results in two stable fixed points and one saddle from a dynamical point of view. Describing the system with a discrete two-state equation, different modes of regular motion have been analyzed. The excitation signal parameters set has been identified for a special type of systems trajectory. Existence of different solutions has been examined in terms of switching signal parameters, that is a frequency and a duty cycle. Obtained numerical results from discrete as well as continuous simulative models have been justified against experimental data from a specially constructed laboratory stand.

1. Introduction

The content of the presented paper focuses on the behavior of an electro-magneto-mechanical system whose the main part is a pendulum. Recent years have shown a growing interest in that kind of systems, it is a result of searching for novel methods of excitation in mechanical engineering as well as pendulums are easy-to-built examples of strongly non-linear mechanical systems.

The experiment setup suggested by Duboshinsky [1–3] involves a pendulum with a magnet suspended above the inductance coil connected to an alternating current source. The orientation of solenoid is perpendicular to the pendulum. The system exhibits quantized modes regarding changes in the system's parameters such as frequency of current or length of the pendulum. The disturbances of these parameters can cause the jumps of system trajectory from one mode to another, those jumps imitate the "quantum jumps" of atomic physics. A similar experiment was conducted by J. Bethenod [2,4]. He reported the phenomenon of growing and sustained oscillations exhibited by a pendulum with a ferromagnetic bob embedded in vary inductance generated by a coil. The pendulum revealed different kinds of behavior in terms of electrical circuit's parameters. The steady-state of oscillations was obtained for an electrical circuit with a predominant reactance. Furthermore, with predominant resistance the oscillations decayed more rapidly than in the case when the coil was unexcited. Sustained oscillations of definite amplitude depended on the reactance of the coil, the voltage and the frequency of excitation as well as internal damping of the mechanical system. Damgov and Popov [5] studied numerically and analytically a kick-excited, self-adaptive pendulum system. Attractor set of the system has been analyzed by multiple bifurcation diagram as well as complex dynamics, evolution and the fractal boundaries of the multiple attractor basins. Siahmakoun et al. [6] investigated experimentally and numerically a driven pendulum in the repulsive magnetic field. They obtained a different kind of attractors and their transformations regarding the system's parameters such as the distance between magnets and frequency of a driven force. Wojna et al. [7] studied a dynamics of a double pendulum driven by external torque, while the lower link of the pendulum has been equipped in a strong magnet acting on the other magnet fixed to the rig's frame. Chaotic and regular motion have been obtained numerically and experimentally and discussed. Numerous of presented regular motions have featured a multiperiodic form. The system of two coupled pendulums subjected to the alternating magnetic field has been examined by Polczyński et al. [8,9]. Numerical and experimental investigation justified the existence of not only a chaotic and regular motion but also quasi-periodicity. Computed basins of attraction have shown the richness of symmetric system's responses in terms of different initial conditions.

2. Experimental setup and physical model

In this section, we present the experimental rig which has been constructed in our department as well as its physical model with forces and moments of forces acting on it. The experimental rig and the physical model of the system are shown in Fig. 1a and Fig. 1b, respectively.

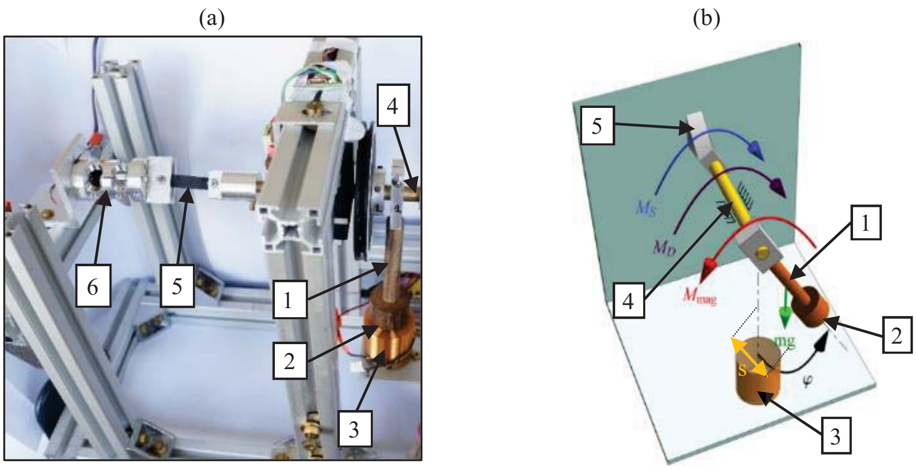

Figure 1. Experimental setup of a single magnetic pendulum (a) and its physical model (b) where: 1 – pendulum, 2 – neodymium magnet (not visible), 3 – electrical coil, 4 – brass pivot, 5 – rubber elastic element and 6 – torque transducer.

The main parts of the system are a single physical pendulum (1) equipped with a neodymium magnet (2) (not visible in Fig.1) at the end of the link and an electrical coil (3) placed underneath. The pendulum is fixed to a brass pivot (4) which is connected with an elastic rubber element (5). The other side of the mentioned element has been fixed to the stationary torque transducer (6). The pendulum's rod is subjected to a gravitational force mg and a torque M_{mag} being a result of repulsive magnetic forces coming from the electric coil. Force mg is put in a center of mass of the pendulum and distance between this center and the axis of rotation is denoted as s. The resistance of the motion is introduced as a torque M_D. It is a sum of all damping factors such as viscous friction, dry friction and internal damping of the elastic element. Moreover, stiffness of the elastic element induces a torque M_S.

The repulsive force generated by the coil is realized by a rectangular current waveform which flows inside the circuit. Fig. 2 pictures particular parameters which are regulated, that is the frequency $f = \frac{1}{\tau}$ and the duty cycle $w = \frac{\tau_{ON}}{\tau} \cdot 100\%$, current's amplitude I was set on 1A.

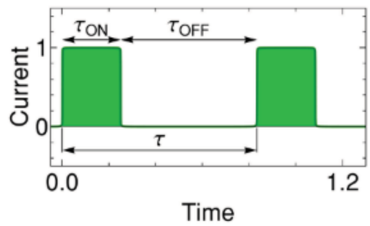

Figure 2. The rectangular current signal flows through the electric coil, where τ is a period of the signal, τ_{ON} is a time when the coil is powered and τ_{OFF} is a time when the coil is switched off.

Angular position of the pendulum has been measured by an incremental optical encoder HEDS-9040#J00, the smallest angular displacement which can be detected is 0.36°. LabVIEW software and NI USB-6341 device were used for the data acquisition process.

3. Mathematical modeling of the system

In this paper two approaches to the systems modeling are presented. The first approach is based on one non-autonomous ordinary differential equation (ODE) describing the system's motion, where the coil's current rectangular signal is modelled with a continuous approximation. The second approach assumes that the coil current signal is discrete, i.e. the coil is instantaneously switched on or off. In this case motion of the system is described with two different autonomous ODEs, which are switched between themselves accordingly to the set frequency and the duty cycle. In this section, we present the conceptions of these two approaches as well as a mathematical model of electromagnetic interaction. Some nomenclature in the section is based on work [5].

3.1. Electromagnetic interaction between a neodymium magnet and an electric coil

The electromagnetic interaction between the magnet and the coil has been investigated previously in our work [8]. The proposed mathematical model was based on experimental data of the torque generated by a steady magnetic field. The complexity of the mentioned model has encouraged us to develop a simpler model to accelerate numerical computation. The simpler model was yielded by the potential analysis. Mathematically, a character of the potential energy generated by the coil-magnet interaction in our system can be approximated by the Gaussian peak function. The mathematical formula used to describe the magnetic potential is as follows

$$V_G(\varphi) = a \exp\left(-\frac{\varphi^2}{b}\right), \tag{1}$$

where coefficient a, b are constant and depend on current amplitude. According to the mechanical definition of the potential, we can calculate torque M_{mag*} acting on the pendulum for steady coil's current as:

$$M_{mag*}(\varphi) = -\frac{\partial V_G}{\partial \varphi} = \frac{2a}{b} \exp\left(-\frac{\varphi^2}{b}\right) \varphi. \tag{2}$$

Fig. 3a depicts the potential of the system. In the case of the one-well potential the system is subjected only to gravitational and elastic element's forces. In the case of the powered coil the two-wells potential is obtained. One can notice that, the significant differences between these two kinds of potentials occur only in so-called "active zone", which is placed between angles $\pm\varphi_A$. Outside of the active zone, the influence of the electromagnetic interaction on the pendulum can be neglected. The experimental measurement and approximation (Eq. 2) of the torque M_{mag*} are shown in Fig. 3b.

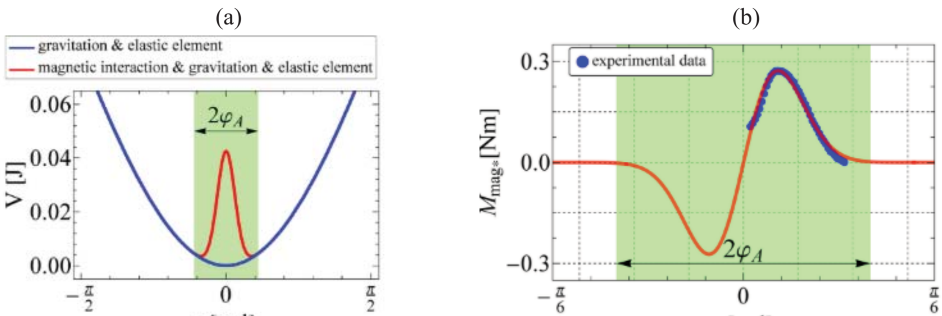

Figure 3. The one-well and two-well potentials of the system (a); The experimental measurement and approximation of the torque M_{mag*} (b).

3.2. Non-autonomous mathematical model

Taking into account the classical mechanics the governing equation of the system can be written as one ODE in a following way

$$J\ddot{\varphi} + c_e\dot{\varphi} + k_e\varphi + mgs\sin\varphi + T_s(\dot{\varphi}) - M_{mag*}I(t) = 0, \quad (3)$$

where J is the pendulum's moment of inertia, c_e and k_e denote viscous damping and stiffness of the elastic element. Term *mgs* stands for a torque of the gravitational force *mg* at arm *s*. Moreover, basing on the experimental measurements we decided to model the damping $T_s(\dot{\varphi})$ which comes from the rolling bearings with the following function:

$$T_s = \left[F_c + (F_s + F_c)\exp\frac{-(\dot{\varphi})^2}{v_s}\right]\tanh\varepsilon\dot{\varphi} + c\dot{\varphi}, \quad (4)$$

where F_c is the value of the simple Coulomb friction, v_s represents so-called Stribeck velocity and the F_s denotes the value of static friction when the pendulum does not move. Term c is viscous damping coefficient, whereas ε is a regularization parameter. Because, the magnetic interaction is possible only when the current flows through the coil, in Eq. 3 the value of M_{mag*} is multiplied by dimensionless current signal $I(t)$ (see Fig. 2) described by the following formula [8]

$$I(t) = \frac{1}{2}\left[1 + \frac{2}{\pi}\arctan\left(\epsilon\sin\left(2\pi f(t + t_0)\right) + i_0\right)\right], \quad (5)$$

where $i_0 = -\sin\left(\frac{\pi - \frac{2\pi w}{100}}{2}\right)$ and $t_0 = \frac{\pi - \frac{2\pi w}{100}}{2\pi f}$. Term w is a percentage duty cycle, f [Hz] stands for the frequency and ϵ is a regularization parameter.

3.3. Discrete mathematical model

The main goal of this approach is to eliminate the continues form of the current signal from the motion's equation. The goal can be achieved by dividing the motion into two different states. Each of the states is described by one autonomous ODE. The occurrences of the relevant states are related to times calculated on the basis of frequency and duty cycle of the current signal. The first state corresponds to the time when the coil is switched off and is governed by the following equation

$$J\ddot{\varphi} + c_e\dot{\varphi} + k_e\varphi + mgs\sin\varphi + T_s(\dot{\varphi}) = 0, \quad (6)$$

whereas the equation of the second state corresponding to the switched-on coil is as follows

$$J\ddot{\varphi} + c_e\dot{\varphi} + k_e\varphi + mgs\sin\varphi + T_s(\dot{\varphi}) - M_{mag*} = 0. \quad (7)$$

As a result, the continues coil current signal has been discretized. Parameters used in Eqs. 6 and 7 have the same description as parameters in the subsection 3.2. The trajectory of the motion is a set of solutions received in numerical integration of the Eqs. 6 and 7. The initial conditions employed to integration process have been taken from the last point of a preceding state's solution. The values of system's parameters were as follow: a=0.0425 [Nm rad], b=0.0181 [rad^2], J=6.787·10^{-4} [kgm^2],

mgs=5.800·10^{-2} [Nm], k_e=1.742·10^{-2} [Nm/rad], c_e=1.282·10^{-4} [Nms/rad], F_c=2.223·10^{-4} [Nm], F_s=4.436·10^{-4} [Nm], φ_A=0.3484 [rad], v_s=0.5374 [rad/s], c=7.369·10^{-5} [kg m2], ε=5.759 [-], ϵ=200 [-].

4. Experimental and numerical investigation of 1-period and one-side pendulum's oscillation

In this section, we present experimental and numerical investigations of one-side oscillations of the pendulum. By one-side oscillations, we mean oscillations of the pendulum without moving through the lower and upper equilibrium positions. Our studies focus on the influence of the duty cycle and frequency of the current signal on the motion. Experimentally, one can observed that for set constant frequency f exists a wide range of the duty cycle w for which the pendulum's oscillation does not change. Fig. 4 displays experimentally obtained phase plots of these same oscillations for various excitation signal's parameters.

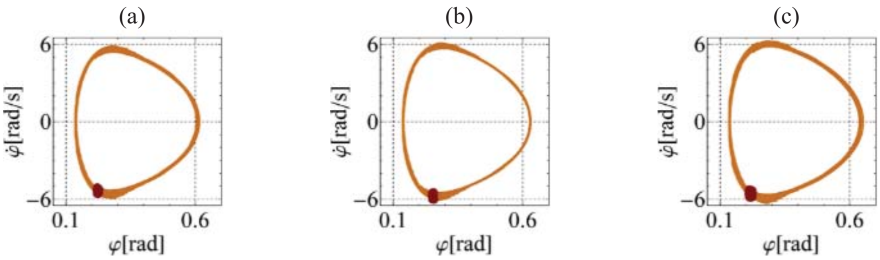

Figure 4. Experimental phase plots and Poincaré sections for a fixed frequency f=3.5 Hz but different duty cycles w: (a) 30%, (b) 60% and (c) 80%.

It is well visible that for a given frequency and different duty cycles it is possible to hold similar oscillations' amplitude, angular velocity and periodicity. In order to understand and explain this behavior we started our analysis from determining the initial conditions, which have to be fulfilled to achieved one-side oscillation. In Fig. 5 we can distinguish two states of pendulum's motion and characteristic points, which pendulum has to cross during oscillation. The first state starts when the pendulum is freely falling from the initial point ($\varphi_0,\omega_0=0$) to the point (φ_k,ω_k) where the coil is switched on what results in the magnetic barrier (blue arrows in Fig. 5a). We call this point "the kick", because the system is "kicked" to the higher energy state (green arrow in Fig. 5a). The system goes to the second state when the pendulum bounces from the magnetic barrier and goes away from it (red arrows in Fig. 5a). Fig. 5b depicts a phase plot of trajectory with colored line segments corresponding to the systems states. Taking into consideration the relations shown in Fig. 5, the 1-period motion can exist only for particular values of boundary conditions (φ_k,ω_k), which used as initial conditions in Eqs. 7 result in the trajectory which crosses the point (φ_0,ω_0=0). The set of these values has been obtained numerically. Frist, a range of search was limited by boundaries following the motion scenario shown in Fig. 5:

(i) the kick must be within the active zone,

(ii) the minimum initial angle φ_0 cannot be smaller than φ_A (yellow line (2) in the Fig.6),

(iii) the initial angle φ_0 cannot provide to potential well escape (blue line (1) in the Fig. 6).

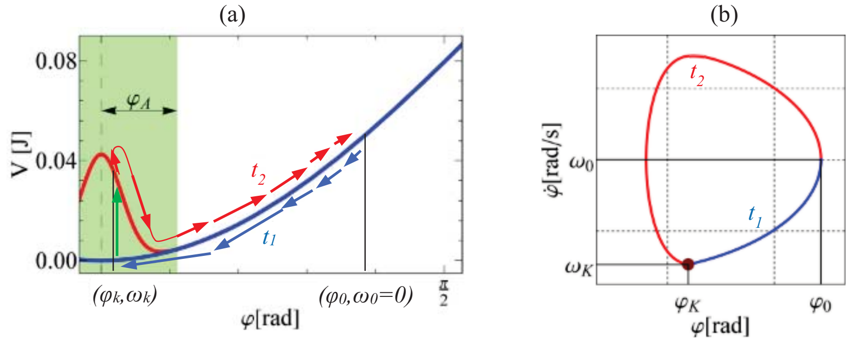

Figure 5. The potential plot (a) and phase plot (b) with characteristic points and stages during one-side pendulum's oscillation.

The obtained set of (φ_k,ω_k) and boundary lines are shown in Fig. 6. For each point (φ_k,ω_k) the time t_1 and t_2 (see Fig. 5a) of the motion's states have been computed. These times are related to the frequency and duty cycle of the current signal $I(t)$ in the following way: $f = 1/(t_1 + t_2)$ and $w = t_2/(t_1 + t_2)$. In Fig. 7, the line labeled as 3 shows the values of w and f that have been computed for the basic scenario shown in the Fig. 5a. However, since we have noticed before, that outside the active zone differences between two states are insignificant, switching off the coil (transition from state 2 to 1) can be performed anywhere outside the active zone. For those same (φ_k,ω_k) one can found the shortest time t_2 (spread from point (φ_k,ω_k) to some point before (φ_0,ω_0)) which corresponds to the minimum duty cycle w – line labeled as 1 in the Fig.7. The similar situation concerns calculating the longest time t_2 (spread from point (φ_k,ω_k) to point after (φ_0,ω_0)) what corresponds to the maximum w – line labeled as 2 in the Fig.7. In other words, the coil can be switched off just after the system leaves the active zone, or just before the system enters it.

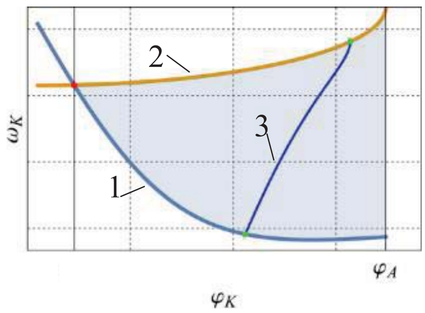

Figure 6. (1), (2) – Boundary conditions; (3) – set of (φ_k,ω_k) fulfilling period-1 motion scenario.

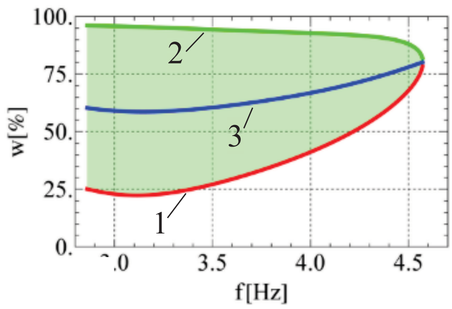

Figure 7. Range of w and f giving 1T and one-side oscillations; (1) – solution described in text; (2) – minimum *w*; (3) – maximum *w*.

Values of frequency and duty cycle get from the green area in Fig. 7 result in period-1 and one-well oscillating solution of the pendulum's motion. The comparison of numerical results to previously presented in Fig.4 solutions is shown in Fig. 8.

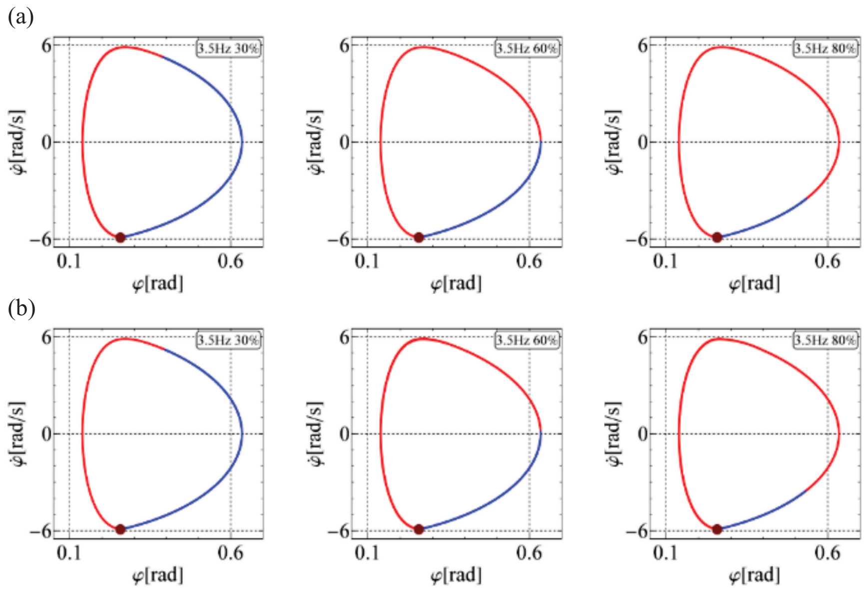

Figure 8. Numerical results of 1T solution calculated by using (a) non-autonomous mathematical model (Eq. 3) and (b) discrete mathematical model (Eqs. 6 and 7).

The comparison of the phase plots has justified that both non-autonomous and discrete models give those same solutions as experiment for fixed frequency 3.5 Hz and three different duty cycles. Numerical investigation have yielded that the amplitude of oscillations increases with decreasing frequency of current signal. Fig. 9 presents behavior of the system for different values of the frequency.

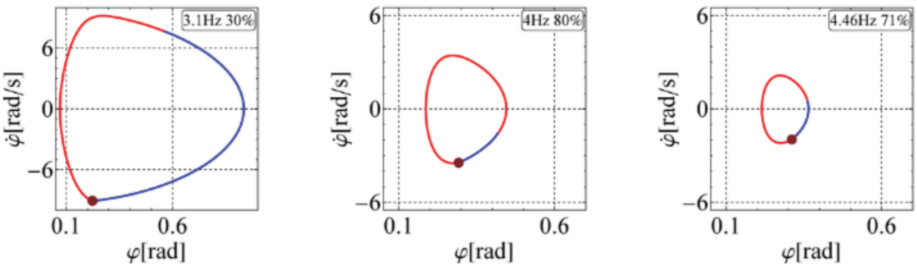

Figure 9. Influence of increasing frequency on oscillation amplitude.

5. Concluding remarks

The nonlinear one-degree-of-freedom system has been investigated numerically and experimentally. The system is composed of a single magnetic pendulum elastically coupled with a fixed base and excited by an alternating magnetic field. Two approaches of mathematical modeling of the system's motion have been presented as well as the model of magnetic interaction. The one-well oscillation has been analyzed in terms of parameters of the current signal: duty cycle and frequency. The numerical computation has yielded a range of duty cycles and frequencies for which the system exhibits period-1 motion. Both non-autonomous and discrete mathematical models provide similar results which are in good agreement with experiment. The work presents promising results which can be used to control so-called "kicked" systems. The future studies will concern more complicated scenarios of the 1-period motion.

Acknowledgments

This work has been supported by the Polish National Science Centre under the grant OPUS 14 No. 2017/27/B/ST8/01330.

References

[1] Penner, D.I., Doubochinski, D.B., Kozakov, M.I., Vermel', A.S., and Galkin, Y. V. Asynchronous excitation of undamped oscillations. *Soviet Physics - Uspekhi* 16 (1973), 158.

[2] Landa, P.S., *Nonlinear Oscillations and Waves in Dynamical Systems*. Springer Netherlands, Dordrecht, 1996.

[3] Doubochinski, D.B. and Tennenbaum, J. Theory and applications of the macroscopic quantization effect in nonlinearly-coupled vibrating systems, in: *1st Euro-Mediterranean Conference on Structural Dynamics and Vibroacoustics*, Marrakech, Marocco, 2013: pp. 23–26.

[4] Kesavamurthy, N. and Rao, G., A. study of Bethenod's phenomenon. *IEEE Transactions on Circuit Theory* 19 (1972), 215–218.

[5] Damgov, V. and Popov, I. "Discrete" Oscillations and multiple attractors in kick-excited systems. *Discrete Dynamics in Nature and Society* 4 (2000), 99–124.

[6] Siahmakoun, A., French, V.A., and Patterson, J. Nonlinear dynamics of a sinusoidally driven

pendulum in a repulsive magnetic field. *American Journal of Physics* 65 (1997), 393–400.

[7] Wojna, M., Wijata, A., Wasilewski, G., and Awrejcewicz, J. Numerical and experimental study of a double physical pendulum with magnetic interaction. *Journal of Sound and Vibration* 430 (2018), 214–230.

[8] Polczyński, K., Wijata, A., Awrejcewicz, J., and Wasilewski, G. Numerical and experimental study of dynamics of two pendulums under a magnetic field. *Proceedings of the Institution of Mechanical Engineers, Part I: Journal of Systems and Control Engineering* 233 (2019), 441–453.

[9] Polczyński, K., Wijata, A., Wasilewski, G., Kudra, G., and Awrejcewicz, J. Modelling and Analysis of Bifurcation Dynamics of Two Coupled Pendulums with a Magnetic Forcing, in: I. Kovacic, S. Lenci (Eds.), *IUTAM Symposium on Exploiting Nonlinear Dynamics for Engineering Systems*, Springer International Publishing, Cham, 2020: pp. 213–223.

Krystian Polczyński, M.Sc. (Ph.D. student): Lodz University of Technology, Department of Automation, Biomechanics and Mechatronics, 1/15 Stefanowskiego Str., 90-924 Łódź, Poland (*krystian.polczynski@edu.p.lodz.pl*). The author gave a presentation of this paper during one of the conference sessions.

Adam Wijata, M.Sc. (Ph.D. student): Lodz University of Technology, Department of Automation, Biomechanics and Mechatronics, 1/15 Stefanowskiego Str., 90-924 Łódź, Poland (*adam.wijata@edu.p.lodz.pl*).

Jan Awrejcewicz, Professor: Lodz University of Technology, Department of Automation, Biomechanics and Mechatronics, 1/15 Stefanowskiego Str., 90-924 Łódź, Poland, (*jan.awrejcewicz@p.lodz.pl*).